the formation of Ti-Ti single bonds.[6] Furthermore, the magnetic moment of **1** (μ_{eff} = 1.81 μ_B), although difficult to interpretate because of the multivalent and polymetallic nature of these compounds, is consistent with the presence of one unpaired electron per molecule. Considering that the anionic fragment of **1** contains one titanium atom bonded to the four amido groups which is probably a d^1 Ti(III), and another which is likely a diamagnetic d^4 Ti(0) atom, the trimetallic Ti(II) frame can reasonably be expected to be diamagnetic. By way of contrast, the V-V distances in the isostructural trivanadium aggregate **3** [ranging from 3.145 (6) to 3.159 (5) Å] are considerably longer and likely not in agreement with the presence of a V-V bond. Assuming a normal d^2 high-spin configuration for the octahedral VCl_4(TMEDA) fragment, the magnetic moment of **3** (μ_{eff} = 5.01 μ_B) indicates that the vanadium atoms of the trinuclear unit should possess a low-spin electronic configuration with less than one unpaired electron per vanadium atom.

There is no doubt that somehow the different electronic configuration of the two metals (d^2 against d^3) should be responsible for the different M-M distances in these two electron-poor clusters.[1] However, in our opinion the low-spin configuration of each vanadium atom in **3** (with two coupled electrons and no V-V bond) makes the existence of a Ti-Ti bond in **1** doubtful, in spite of the short "bonding" distance.

Consistent with this rationale, the cleavage of the trimetallic frames was easily achieved with both **1** and **3** via simple treatment with pyridine at room temperature, forming the monomeric $(pyridine)_4MCl_2$ [M = Ti,[7a] V[7b]] as deep blue and deep red crystalline solids, respectively.

Acknowledgment. This work was supported by the Natural Sciences and Engineering Research Council of Canada (operating grant) and the donors of the Petroleum Research Fund, administered by the American Chemical Society. We are indebted to the Nederlandse Organisatie voor Wetenschappelijk Onderzoek (NWO) for providing a visiting scholarship (J.J.H.E.) and to Dr. B. Vincent (Molecular Structure Corp., Woodlands, TX) for solving the crystal structure of **3**.

Supplementary Material Available: Tables listing crystallographic data, atomic positional parameters, anisotropic thermal parameters, and complete bond distances and angles for **1** and **3**, an ORTEP diagram (Figure 1S) of the $[VCl_4(TMEDA)]^-$ anion in **3**, and a fully labeled ORTEP for the cation **3** (32 pages); tables of observed and calculated structure factors for **1** and **3** (70 pages). Ordering information is given on any current masthead page.

Department of Chemistry
University of Ottawa
Ottawa, Ontario K1N 6N5, Canada

Jilles J. H. Edema
Robbert Duchateau
Sandro Gambarotta*
Corinne Bensimon

Received January 24, 1991

[Fe(4-imidazoleacetate)$_2$]·2CH$_3$OH: A 2D Antiferromagnetic Iron(II) System Exhibiting 3D Long-Range Ordering with a Net Magnetic Moment at 15 K

Cooperative magnetic phenomena are well-known in solid-state materials but rare in molecular systems. Although substantial efforts have focused on the preparation of ferro- or ferrimagnetic molecular compounds exhibiting long-range magnetic ordering during the past few years, the transition temperature of the ferromagnetic molecular compounds reported so far is extremely low.[1,2] On the other hand, some antiferromagnetic substances exhibit weak ferromagnetism at low temperature resulting from a canting of the spins.[3] Although uncommon, such a situation may occur either in linear chain systems when magnetic interactions between next nearest neighbors occur or in two- or three-dimensional materials.[4] Among this class of compounds, the layered complexes of 1,2,4-triazole with divalent metal thiocyanates,[5] although exhibiting canted spin structures quite similar to that reported in this work, are characterized by low ordering temperature (3-6 K) and hidden canting. The title compound, [Fe(4-imidazoleacetate)$_2$]·2CH$_3$OH, exhibits a net magnetic moment below 15 K, the highest 3D ordering temperature reported so far for a molecular compound characterized by a canted spin structure.

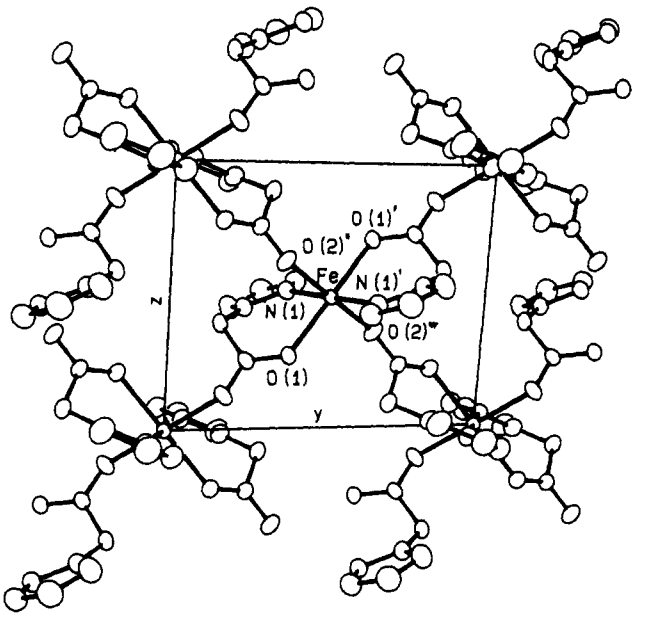

Figure 1. Projection of the unit cell of the [Fe(4-imidazoleacetate)$_2$]·2CH$_3$OH (1) complex molecule onto the *yz* plane. For clarity, the methanol molecules have been omitted.

Reaction of a 2:1 molar ratio of sodium 4-imidazoleacetate (Sigma) and ferrous acetate tetrahydrate[6] in deoxygenated methanol for 12 h affords white microcrystals of [Fe(4-imidazoleacetate)$_2$]·2CH$_3$OH (**1**) in 92% yield. Colorless single crystals suitable for X-ray diffraction study[7] were obtained by slow interdiffusion of deoxygenated methanolic solutions of sodium

(1) Miller, J. S.; Epstein, A. J.; Reiff, W. M. *Chem. Rev.* **1988**, *88*, 201.
(2) (a) Caneschi, A.; Gateschi, D.; Renard, J. P.; Rey, P.; Sessoli, R. *Inorg. Chem.* **1989**, *28*, 2940. (b) Nakatani, K.; Carriat, J. Y.; Journeaux, Y.; Khan, O.; Lloret, M.; Renard, J. P.; Pey, Y.; Sletten, J.; Verdaguer, M. *J. Am. Chem. Soc.* **1989**, *111*, 5739.
(3) Moriya, T. In *Magnetism*; Rado, G. T., Suhl, H., Eds.; Academic Press: New York, 1963; Vol. 1, Chapter 3.
(4) Carlin, R. L. *Magnetochemistry*; Springer-Verlag: Berlin, 1986; Chapters 6 and 7.
(5) References 130-137 in Chapter 7 of ref 4.
(6) Rhoda, R. N.; Fraioli, A. V. *Inorg. Synth.* **1953**, *4*, 159.
(7) Crystals of complex **1** belong to the monoclinic system, space group $P2_1/c$, with a 9.842 (2) Å, b = 9.522 (2) Å, c = 8.144 (2) Å, β = 96.74 (2)°, V = 763 (1) Å^3, Z = 2, and d_{measd} = 1.57 (4) g cm^{-3}. Diffraction data were collected at −6 °C to a 2θ(Mo) maximum of 30° by procedures described elsewhere[9] using an Enraf-Nonius CAD 4 diffractometer with graphite-monochromated Mo Kα radiation. A total of 4448 reflections were recorded. A linear decay correction (total intensity loss 1.2%) was applied to the data as well as an absorption correction using the numerical method of Coppens.[10] Reflections were corrected for Lorentz and polarization effects,[11] 2074 of which with $I > 2\sigma$ were used in subsequent calculations. The structure was solved by using the heavy-atom method.[12] All non-hydrogen atoms were refined anisotropically. All hydrogen atoms were included in the calculations at a fixed distance of 0.95 Å with a mean isotropic temperature factor U = 0.065 Å^2. The atomic scattering factors used were those proposed by Cromer and Waber[13] with anomalous dispersion effects.[14] The final full-matrix least-squares refinement, minimizing $\sum w(|F_o| - |F_c|)^2$, converged to $R = \sum||F_o| - |F_c||/\sum|F_o| = 0.031$ and $R_w = [(\sum w||F_o| - |F_c||)w]/[(\sum|F_o|)w] = 0.043$ with a weighting scheme $w = 1/[\sigma^2(F) + 0.005F^2]^{1/2}$. The goodness of fit was S = 1.01.

0020-1669/91/1330-3587$02.50/0

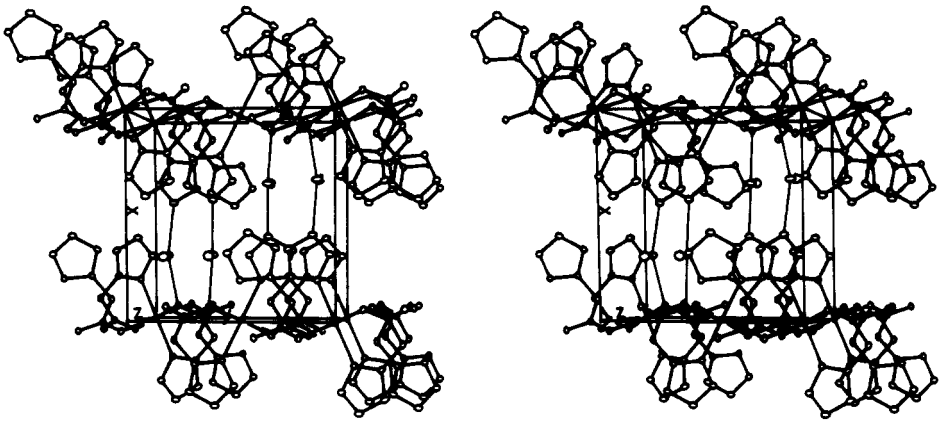

Figure 2. Stereoview of the unit cell of **1** showing the interlayer contacts through the methanol molecules.

4-imidazoleacetate and ferrous acetate tetrahydrate.

The complex molecule shown in Figure 1 is located on a crystallographic inversion center in the unit cell. Each molecule includes two trans 4-imidazoleacetato ligands coordinated through the O(1) acetato oxygen and N(1) nitrogen donors. Two trans O(2) acetato oxygen donors arising from the 4-imidazoleacetato ligands of adjacent complex molecules supplement the iron(II) coordination octahedron.

The iron ligand environment can be described as a rhombically distorted octahedron, the basal plane of which includes the N(1) and N(1)′ imidazole nitrogens and O(2)″ and O(2)‴ acetate oxygen atoms 2.145 (1) and 2.132 (1) Å away from the iron center, respectively. The O(1) and O(1)′ oxygen donors situated at the apices are separated from the iron atom by a distance of 2.188 (1) Å. This situation results in a slightly elongated octahedron. The N(1)···O(1) bite of the 4-imidazoleacetato chelate tilts the O(1)–O(1)′ axis ca. 8° from the normal to the basal plane. The angle between the planes of the imidazole ring and acetato group of the 4-imidazoleacetato ligand is 52.23 (4)°, and the N(1)–C(3)–C(4)–C(5) and C(3)–C(4)–C(5)–O(1) torsion angles are 57.62 (4) and 47.14 (4)°, respectively.

Each molecule of **1** is linked to four neighboring molecules through acetato bridges, affording intertwined linear chains along [011] and [01$\bar{1}$] that result in sheets parallel to *yz*. The intrachain Fe···Fe distance resulting from these acetato bridges is 6.265 (3) Å. Two adjacent ferrous sites being related by a glide plane, the angle between the O(2)″–Fe–O(2)‴ directions of adjacent molecules in a sheet is equal to 94.65 (4)°, while that between the O(1)–Fe–O(1)′ directions is equal to 74.96 (4)°. The crystal packing (Figure 2) results from a network of hydrogen bonds interlinking the sheets via the O(3) atom of the lattice methanol molecules, which are bonded to O(1) through the H(6) methanol hydrogen atom (2.792 (2) Å) and to N(2) ($x-1, y, z$) through the H(2) imidazole hydrogen atom (2.743 (2) Å). These O(3)–H(6)···O(1) and O(3)···H(2)–N(2) contacts afford doubly hydrogen-bonded sheets along [100]. This packing results in intersheet Fe···Fe distances of 9.843 (2) Å.

The iron is in the high-spin ferrous state as indicated by the magnetic moment of 5.2 μ_B at 300 K (χT = 3.38 emu mol^{-1} K). The temperature dependence of the magnetic susceptibility studied in the 1.7–100 K range and a 0.5-kOe applied magnetic field is displayed in Figure 3 as χ versus T and χT versus T. The χT product decreases monotonically from 2.99 emu mol^{-1} at 100 K to 1.90 emu mol^{-1} K at 20 K. This decrease is related to both antiferromagnetic interactions and a spin–orbit coupling effect, well documented in the case of octahedral iron(II). A magnetic phase transition occurs at 15 K, resulting in a χT maximum of 27.37 emu mol^{-1} K. Ac susceptibility measurements performed below 20 K show an out-of-phase signal characteristic of a three-dimensional ferromagnetic (or weak ferromagnetic) ordering. Magnetization measurements performed up to 30 kOe show that, in the paramagnetic region ($T > 17$ K), the magnetization varies linearly with the applied magnetic field up to ca. 15 kOe. At 4.2 K, the field dependence of the magnetization departs from linearity

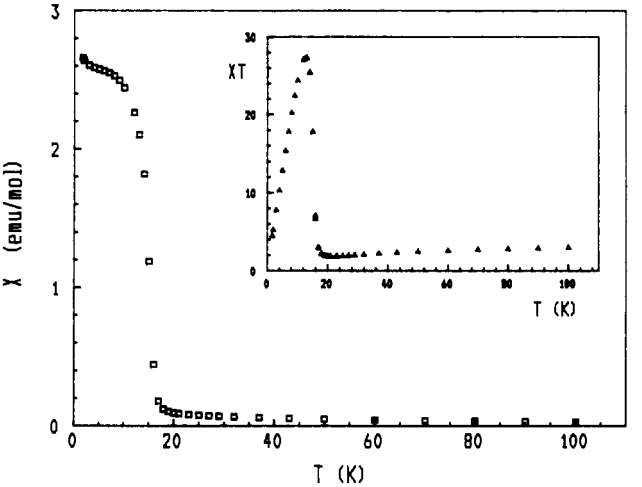

Figure 3. Variation of the magnetic susceptibility and χT product (insert) of a powdered sample of **1** with temperature at 0.5 kOe.

above 2 kOe, but saturation is not reached, even at 30 kOe (Figure 4). When the magnetic field is cycled between +30 and −30 kOe, a characteristic hysteresis loop is obtained with a remanent magnetization of 0.22 μ_B and a coercive field of 6.2 kOe (Figure 4). These results clearly show that (i) the saturation of the magnetization occurs at a value slightly lower than 1 μ_B, far away from the theoretical value for an $S = 2$ spin system (4 μ_B), (ii) the net magnetic moment at zero field agrees with a canted spin structure, and (iii) the very high coercive field observed is unprecedented for a molecular material. Finally, these observations agree with the presence of a weak ferromagnetic ground state.

The three-dimensional ordering of this homometallic lattice is confirmed by Mössbauer spectroscopy (Figure 5). Above 17 K, **1** affords a quadrupole-split doublet characteristic of high-spin iron(II) (isomer shift δ = 1.26 mm s^{-1} relative to metallic iron at 300 K, quadrupole splitting ΔE_Q = 3.46 mm s^{-1} at 80 K). Well-resolved Zeeman spectra are obtained below 15 K, indicating a saturation value of the effective internal field of ca. 150 kG at the Mössbauer nucleus and a positive V_{zz} component of the electric field gradient.[8]

(8) Kündig, W. *Nucl. Instrum. Methods* **1967**, *48*, 219.
(9) Mosset, A.; Bonnet, J.-J.; Galy, J. *Acta Crystallogr., Sect. B: Struct. Crystallogr. Cryst. Chem.* **1977**, *B33*, 2639.
(10) Coppens, P.; Leiserowitz, L.; Rabinovich, D. *Acta Crystallogr.* **1965**, *18*, 1035.
(11) Frenz, B. A. *SDP—Structure Determination Package*; Enraf-Nonius: Delft, Holland, 1982.
(12) Sheldrick, G. M. In *Crystallographic Computing 3*; Sheldrick, G. M., Krüger, C., Goddard, R., Eds.; Oxford University Press: Oxford, England, 1985; pp 175–179.
(13) Cromer, D. T.; Waber, J. T. *International Tables for X-ray Crystallography*; Kynoch Press: Birmingham, England, 1974; Vol. IV, Table 2.2.B, pp 99, 101.

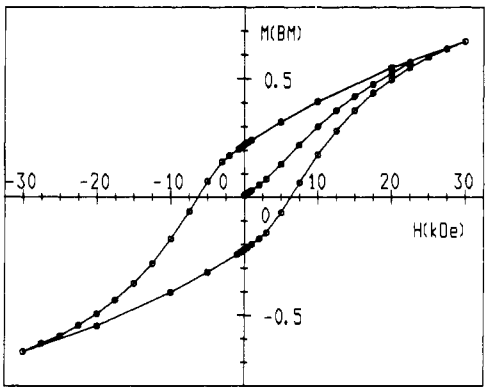

Figure 4. Field dependence of the magnetization of a powdered sample of **1** at 4.2 K.

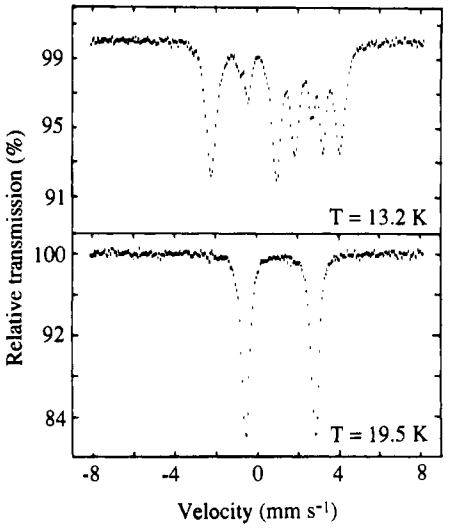

Figure 5. Mössbauer spectra of **1** at 19.5 and 13.2 K.

A close examination of the X-ray molecular structure allows us to explain the origin of the weak ferromagnetism observed. The electronic structure of the iron(II) ion results from competing effects between spin coupling and local distortion. Due to the angle between the O(2)″–Fe–O(2)‴ directions of adjacent molecules in a sheet (94.65 (4)°), the relative orientations of adjacent ferrous coordination polyhedra result in the presence of two spin sublattices. The competition between this local effect and the antiferromagnetic exchange interaction mediated by the acetato bridges between adjacent ferrous ions affords a magnetic ground state within each layer. Finally, it can be assumed that the interactions between these magnetic layers through the hydrogen-bonding network described in Figure 2 promote the three-dimensional ferromagnetic ordering observed.

Work in progress includes high-field magnetization measurements, a frequency-dependent ac magnetic susceptibility study, and specific heat and neutron diffraction powder diagram studies.

Acknowledgment. The CNRS and the National Hellenic Research Foundation are acknowledged for partial support of this work. M.-A.M.-L. thanks the Commission of European Communities (Science Program) for a doctoral fellowship.

Supplementary Material Available: An ORTEP view of the complex molecule of **1** displaying numbering of the atoms and tables of crystallographic data, atomic positional and thermal parameters, bond distances and angles, components of the anisotropic temperature factors, and deviations of atoms from their least-squares planes (8 pages); a listing of observed and calculated structure factor amplitudes (13 pages). Ordering information is given on any current masthead page.

(14) Cromer, D. T. *International Tables for X-ray Crystallography*; Kynoch Press: Birmingham, England, 1974; Vol. IV, Table 2.3.1, p 149.

(15) Unité No. 8241 liée par conventions à l'Université Paul Sabatier et à l'Institut National Polytechnique de Toulouse.

Laboratoire de Chimie de Coordination du CNRS[15]
205 route de Narbonne
31077 Toulouse Cedex, France
Maria-Angeles Martinez-Lorente
Jean-Pierre Tuchagues*

National Research Center Demokritos
153 10 Aghia Paraskevi
Attiki, Greece
Vasili Pétrouléas

Centre d'Elaboration des Matériaux et d'Etudes Structurales
29 rue Jeanne Marvig
31055 Toulouse Cedex, France
Jean-Michel Savariault

Groupe des Matériaux Inorganiques
EHICS
1 rue Blaise Pascal
67008 Strasbourg, France
Richard Poinsot
Marc Drillon

Received March 22, 1991

Dicarbollide Complexes of Thallium: Structural and ^{11}B NMR Studies

Recently there has been a great deal of interest in organometallic compounds involving the heavier Group 13 elements, with particular relevance to the bonding in monovalent complexes of thallium and indium.[1] Dicarbollide complexes incorporating thallium(I) were first prepared by Stone[2] and have been used extensively as synthons in metallacarborane chemistry.[3] In order to further explore the structural chemistry of thallium dicarbollide complexes, the anionic thallacarborane [*closo*-3,1,2-$TlC_2B_9H_{11}$]$^-$ (**1**) was prepared as the (PPN)[4] salt by anhydrous metathesis of (Tl)**1**[2] with [PPN]$^+$Cl$^-$ in CH_3CN. This monothallacarborane complex, [PPN]**1**, is very soluble in coordinating solvents such as THF[4] or CH_3CN, in marked contrast to the dithallium precursor. The solid-state structure of [PPN]**1** was established by a single-crystal X-ray diffraction study,[5] which showed well-

(1) (a) Janiak, C.; Hoffmann, R. *J. Am. Chem. Soc.* **1990**, *112*, 5924. (b) Janiak, C.; Hoffmann, R. *Angew. Chem., Int. Ed. Engl.* **1989**, *28*, 1688. (c) Beachley, O. T., Jr.; Churchill, M. R.; Fettinger, J. C.; Pazik, J. C.; Victoriano, L. *J. Am. Chem. Soc.* **1986**, *108*, 4666 and references contained therein.

(2) Spencer, J. L.; Green, M.; Stone, F. G. A. *J. Chem. Soc., Chem. Commun.* **1972**, 1178.

(3) See, for example: (a) Manning, M. J.; Knobler, C. B.; Hawthorne, M. F. *J. Am. Chem. Soc.* **1988**, *110*, 4458. (b) Do, Y.; Knobler, C. B.; Hawthorne, M. F. *J. Am. Chem. Soc.* **1987**, *109*, 1853.

(4) (PPN)$^+$Cl$^-$ = bis(triphenylphosphoranylidene)ammonium chloride. THF = tetrahydrofuran.

(5) (PPN)**1**: (a) Pale yellow parallelepiped single crystals from a $CH_3CN/(C_2H_5)_2O$ solution. (b) a = 15.006 (2) Å, b = 18.964 (2) Å, c = 16.178 (2) Å, β = 112.231 (3)°, V = 4258 Å^3, Z = 2 (two dimeric anions and four cations per unit cell), space group $P2_1/n$, 3509 independent reflections with $I > 3\sigma(I)$, R (R_w) = 0.067 (0.077). (c) Diffraction data were collected at 298 K in the θ–2θ scan mode for 7519 unique reflections having $2\theta < 50°$ on a diffractometer constructed by Prof. C. E. Strouse of UCLA using graphite-monochromated Mo Kα radiation. (d) Data were corrected for Lorentz, polarization, and absorption effects. Atoms were located by use of the heavy-atom method, and SHELX76 was used for structure factor calculations and full-matrix least-squares refinement.

0020-1669/91/1330-3589$02.50/0